J|A|C|S ARTICLES

Published on Web 06/11/2009

Molecular and Morphological Influences on the Open Circuit Voltages of Organic Photovoltaic Devices

M. Dolores Perez,[†] Carsten Borek,[†] Stephen R. Forrest,*[,‡] and Mark E. Thompson*[,†]

Department of Chemistry, University of Southern California, Los Angeles, California 90089, and Departments of Electrical Engineering and Computer Science, Physics and Materials Science and Engineering, University of Michigan, Ann Arbor, Michigan 48109

Received January 31, 2009; E-mail: met@usc.edu; stevefor@umich.edu

Abstract: We explore the dependence of the dark current of C_{60}-based organic photovoltaic (OPV) cells on molecular composition and the degree of intermolecular interaction of several molecular donor materials. The saturation dark current density, J_S, is an important factor in determining the open circuit voltage, V_{oc}. The V_{oc} values of OPVs show a strong inverse correlation with J_S. Donor materials that show evidence for aggregation in their thin-film absorption spectra and polycrystallinity in thin film X-ray diffraction result in a high dark current, and thus a low V_{oc}. In contrast, donor materials with structures that hinder intermolecular π-interaction give amorphous thin films and reduced values of J_S, relative to donors with strong intermolecular π-interactions, leading to a high V_{oc}. This work provides guidance for the design of materials and device architectures that maximize OPV cell power conversion efficiency.

Introduction

The recent growing demand for cost-effective renewable energy has generated considerable interest in the field of organic solar cells. Organic photovoltaic (OPV) cells have the potential to substantially lower costs for solar energy conversion, given their expected low materials and fabrication costs. For OPVs to make a meaningful contribution to meeting our overall energy needs, however, their efficiencies need to be significantly improved from current values that are in the range of 5−6%.[1,2] This is compared to inorganic solar cell efficiencies of >20%. A basic understanding of the processes that control and limit the operation of solar cells is crucial to their improvement and can serve as a guide for identification of new materials for high performance devices. A key limitation in OPVs to date is their low open circuit voltages (V_{oc}), which is typically less than half of the incident photon energy. Here we explore the relationship between materials properties and the open circuit voltage.

OPVs harvest energy on the basis of exciton generation and transport. Photogenerated excitons can form in either the electron donor (D) or acceptor (A) layer in a bilayer cell, as shown in Scheme 1. They subsequently diffuse to the D/A interface where they dissociate to give a free hole and electron that are eventually collected at the contacts. The solar power conversion efficiency (η) is the ratio of the electrical power produced by the cell to the incident power of the solar irradiation (P_o). The power conversion efficiency is the product of the short circuit current (J_{SC}), open circuit voltage (V_{oc}), and the fill factor (FF), following $\eta = J_{SC}V_{oc}FF/P_o$. A number of factors affect the photocurrent, including the light intensity, optical density of the cell, the degree of overlap between the D and A layer absorption spectra with that of the emission spectrum of the sun, the exciton diffusion lengths in the D and A layers, and the charge separation efficiency at the D/A interface. The FF is related to the cell series resistance (R_s), while V_{oc} depnds on the choice of the D/A material combination, electrode material, light intensity, and temperature of operation.[3−7] Additionally, different donor and acceptor materials combinations influence V_{oc}. Specifically, several studies have demonstrated a dependence of V_{oc} on the energy difference between the highest occupied molecular orbital (HOMO) energy of the donor and the lowest unoccupied molecular orbital (LUMO) energy of the acceptor; a difference called the D/A interface energy gap (ΔE_{DA}, Scheme

Scheme 1

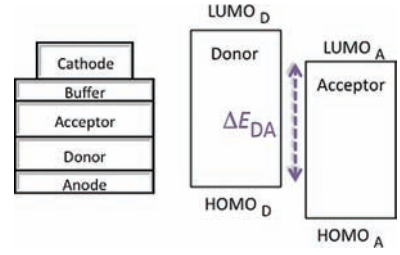

[†] University of Southern California.
[‡] University of Michigan.

(1) Xue, J. G.; Uchida, S.; Rand, B. P.; Forrest, S. R. *Appl. Phys. Lett.* **2004**, *84*, 3013–3015.
(2) Peet, J.; Kim, J. Y.; Coates, N. E.; Ma, W. L.; Moses, D.; Heeger, A. J.; Bazan, G. C. *Nat. Mater.* **2007**, *6*, 497–500.
(3) Mihailetchi, V. D.; Blom, P. W. M.; Hummelen, J. C.; Rispens, M. T. *J. Appl. Phys.* **2003**, *94*, 6849–6854.
(4) Koster, L. J. A.; Mihailetchi, V. D.; Ramaker, R.; Blom, P. W. M. *Appl. Phys. Lett.* **2005**, *86*, 123509.
(5) Mandoc, M. M.; Koster, L. J. A.; Blom, P. W. M. *Appl. Phys. Lett.* **2007**, *90*, 133504.
(6) Liu, J.; Y., S.; Yang, Y. *Adv. Funct. Mater.* **2001**, *11*, 420–424.
(7) Rand, B. P.; Burk, D. P.; Forrest, S. R. *Phys. Rev. B* **2007**, *75*, 115327.

1).[7−14] However, under normal operating conditions (i.e., room temperature and 1 sun intensity illumination) the experimental values for V_{oc} can differ from those inferred from ΔE_{DA} for some materials systems. This disparity is a result of the electronic properties of the donor, acceptor and the D/A interface. A more thorough understanding of molecular materials properties that influence V_{oc} is important to develop new OPV materials that lead to a high V_{oc}.

Here, we identify a correspondence between molecular composition and crystal morphology and the open circuit voltage in small-molecule-based OPVs. Data are presented for several OPVs in which different donor materials are used along with a common acceptor (i.e., C_{60}) to highlight the most important factors governing this relationship.

Physical Origin of the Open Circuit Voltage

The generalized Shockley equation, eq 1,[15,16] describes the current density (J) vs voltage characteristics of organic solar cells:

$$J = \frac{R_p}{R_s + R_p}\left\{J_s\left[\exp\left(\frac{q(V - JR_s)}{nkT}\right) - 1\right] + \frac{V}{R_p}\right\} - J_{ph}(V) \quad (1)$$

Here, R_p is the parallel resistance, J_S is the saturation current density, q is the fundamental charge, n is the diode ideality factor, and $J_{ph}(V)$ is the voltage-dependent photocurrent density. For solar cells with minimal leakage current ($R_p \gg R_s$), eq 1 can be simplified to

$$J = J_S\left[\exp\left(\frac{q(V - JR_s)}{nkT}\right) - 1\right] - J_{ph}(V) \quad (2)$$

The first term describes the thermally generated current that is typically dominated by recombination at the D/A interface, and the second term accounts for photogenerated carriers, $J_{ph}(V)$. Under open circuit conditions ($J = 0$, $V = V_{oc}$), the rate of carrier recombination equals the rate of optical carrier generation. Assuming open circuit conditions, a short circuit current of $J_{SC} = J_{ph}(0) \gg J_S$, and a low series resistance, eq 2 can be solved to give eq 3, in which V_{oc} is given by[7,17,18]

$$V_{oc} \approx \frac{nkT}{q}\ln\left(\frac{J_{SC}}{J_S}\right) \quad (3)$$

Hence, at a given J_{SC} a low dark current (J_S) results in a high V_{oc}. Insight can be gained by examining the origin of J_S, which is the current resulting from carriers generated thermally at the D/A interface, or originating within the film bulk. The saturation current due to interface charge generation has been shown to vary exponentially with ΔE_{DA}, which is represented by eq 4 for systems where J_S is dominated by recombination ($n \approx 2$), as observed for most OPVs.[7,15,16,19]

$$J_S = J_{SO}\exp\left(\frac{-\Delta E_{DA}}{2nkT}\right) \quad (4)$$

The factor of 2 accounts for the thermal generation of both an electron and hole at the D/A heterointerface, giving an activation energy of $\Delta E_{DA}/2$ for the process. The magnitude of J_{SO} depends on a number of materials properties that determine the carrier generation/recombination rate, independent of the energy barrier, ΔE_{DA}. Materials properties affecting the magnitude of J_{SO} include the reorganization energy for D→A electron transfer, the intermolecular overlap at the D/A interface, the layer electrical conductivities, the area of the D/A interface, and the density of states at the HOMO and LUMO energies of the D and A materials.

Substitution of eq 4 into eq 3 yields

$$V_{oc} = \frac{nkT}{q}\ln\left(\frac{J_{SC}}{J_{SO}}\right) + \frac{\Delta E_{DA}}{2q} \quad (5)$$

Equation 5 suggests a linear dependence of V_{oc} on the interface energy gap and a logarithmic dependence on J_{SC} and light intensity ($J_{SC} \propto P_0$), as experimentally observed for both bulk heterojunctions[3,20,21] and lamellar OPVs.[7,22,23] A linear correlation of V_{oc} to ΔE_{DA} has been reported previously for several materials systems.[7,13,14] Here, ΔE_{DA} is the thermal activation energy for charge separation at the D/A interface, such that at low temperatures the measured V_{oc} approaches $\Delta E_{DA}/2$, as recently reported by Rand, et al. for vapor deposited OPVs.[7] Note that eq 5 is similar to, but with important physical implications different from that recently reported by Potscavage, et al.[24] The equation reported in their publication has two different ideality factors (n and n') and suggests a scaling of V_{oc} by $\Delta E_{DA}/q$, rather than $\Delta E_{DA}/2q$, in contrast to what has been observed experimentally. In addition, Potscavage, et al., have assumed that J_{SO} is constant for different D/A pairs, which is inconsistent with the data presented below.

In this work, we study the relationship of various materials combinations to V_{oc} as expressed by eq 5. In particular, we explore the role of J_{SO} in controlling the V_{oc}, and what molecular properties affect the magnitude of J_{SO}. The intermolecular overlap in the donor and acceptor layers and at the D/A interface,

(8) Brabec, C. J.; Cravino, A.; Meissner, D.; Sariciftci, N. S.; Fromherz, T.; Rispens, M. T.; Sanchez, L.; Hummelen, J. C. *Adv. Funct. Mater.* **2001**, *11*, 374–380.
(9) Gadisa, A.; Svensson, M.; Andersson, M. R.; Inganas, O. *Appl. Phys. Lett.* **2004**, *84*, 1609–1611.
(10) Kooistra, F. B.; Knol, J.; Kastenberg, F.; Popescu, L. M.; Verhees, W. J. H.; Kroon, J. M.; Hummelen, J. C. *Org. Lett.* **2007**, *9*, 551–554.
(11) Mutolo, K. L.; Mayo, E. I.; Rand, B. P.; Forrest, S. R.; Thompson, M. E. *J. Am. Chem. Soc.* **2006**, *128*, 8108–8109.
(12) Sarangerel, K.; Ganzorig, C.; Fujihira, M.; Sakomura, M.; Ueda, K. *Chem. Lett.* **2008**, *37*, 778–779.
(13) Scharber, M. C.; Wuhlbacher, D.; Koppe, M.; Denk, P.; Waldauf, C.; Heeger, A. J.; Brabec, C. L. *Adv. Mater.* **2006**, *18*, 789–xxx.
(14) Vandewal, K.; Gadisa, A.; Oosterbaan, W. D.; Bertho, S.; Banishoeib, F.; Van Severen, I.; Lutsen, L.; Cleij, T. J.; Vanderzande, D.; V., M. J. *Adv. Funct. Mater.* **2008**, *18*, 2064–2070.
(15) Fahrenbruch, A. L.; Aranovich, J. *Solar Energy Conversion—Solid-State Physics Aspects*; Springer-Verlag: Berlin, Heidelberg, New York, 1979; Vol. 31.
(16) Bube, H. R.; Fahrenbruch, A. L. *Book Title* Academic: New York, 1981, p 163.
(17) Li, N.; Lassiter, B. E.; Lunt, R. R.; Wei, G.; Forrest, S. R. *Appl. Phys. Lett.* **2009**, *94*, 023307–3.
(18) Sze, S. M. *Physics of Semiconductor Devices*, 2nd ed.; Wiley-Interscience: New York, 1981.
(19) Würfel, P. *Physics of Solar Cells: From Principles to New Concepts*; Wiley-VCH: Weinhem, 2005.
(20) Schilinsky, P.; Waldauf, C.; Brabec, C. J. *Appl. Phys. Lett.* **2002**, *81*, 3885.
(21) Riedel, I.; Parisi, J.; Dyakonov, V.; Lutsen, L.; Vanderzande, D.; Hummelen, J. C. *Adv. Funct. Mater.* **2004**, *14*, 38.
(22) Peumans, P.; Yakimov, A.; Forrest, S. R. *J. Appl. Phys.* **2003**, *93*, 3693–3723.
(23) Signerski, R. *J. Non-Cryst. Sol.* **2008**, *354*, 4465.
(24) Potscavage, J. W. J.; Yoo, S.; Kippelen, B. *Appl. Phys. Lett.* **2008**, *93*, 193308–3.

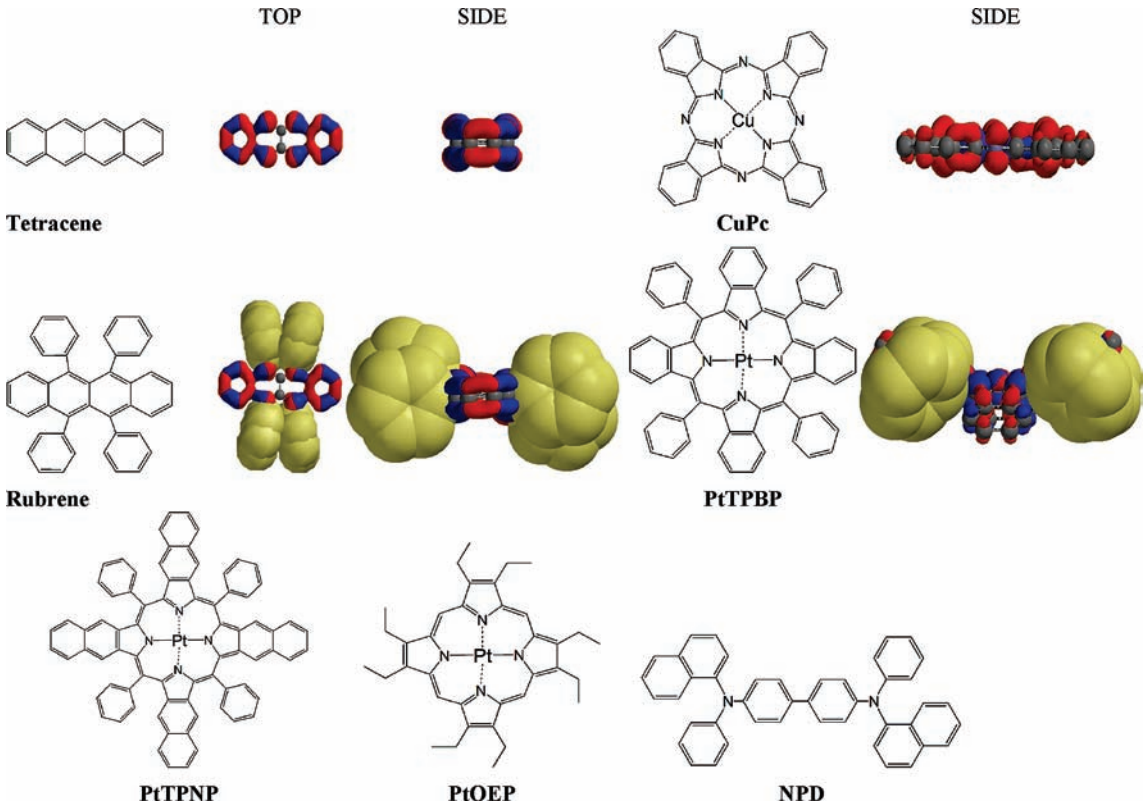

Figure 1. Molecular structures of donors and the corresponding HOMO (blue) and LUMO (red) electron density distributions for tetracene, rubrene, CuPc, and PtTPBP. Phenyl rings are shown as yellow space-filling surfaces.

Table 1. Dark and Light Characteristic Parameters for All Devices with the Structure ITO/Donor/C_{60} (400 Å)/BCP (100 Å)/Al (1000 Å)

donor (Thickness, Å)	J_S (μA/cm^2)	V_{oc} (V)	J_{SC} (mA/cm^2)	FF	η (%)	n
SubPc (130)	3.2×10^{-6}	0.97	3.36[11]	0.57[11]	2.1[11]	1.8[11]
rubrene (200)	2.5×10^{-3}	0.92	2.35	0.43	0.92	2.1
NPD (100)	5.17×10^{-3}	0.85	2.35	0.47	0.93	2.5
PtTPBP (150)	0.020	0.69	4.5	0.63	1.9	2.1
tetracene (600)	0.077	0.55	1.8	0.54	0.53	2.2
PtOEP (150)	0.081	0.52	1.6	0.59	0.49	2.0
PdTPBP[a] (150)	0.24	0.61	2.41	0.62	1.8	2.4
CuPc (400)	1.1	0.48	5.5	0.60	1.6	2.0
PtTPNP (120)	18	0.31	4.2	0.51	0.66	2.2

[a] Illumination intensity = 0.5 suns.

as well as film morphology influence J_{SC} by limiting the exciton diffusion length, as well as by impacting the energetics and kinetics of charge transfer at the interface, thus affecting J_{SO}. Clearly, to achieve the maximum possible V_{oc} for a given D/A pair, J_{SO} must be minimized.

Results and Discussion

A number of photovoltaic devices with the structure ITO/donor/C_{60} (400 Å)/bathocuproine (BCP) (100 Å)/Al (1000 Å), using the donor materials in Figure 1, were fabricated, and both the light and dark performance characteristics were studied (see Experimental Section).

The dark current $J-V$ characteristics were fit to eq 1 to extract n and J_S (Table 1). The parameters, J_{SC}, V_{oc}, FF, and η, were obtained under simulated 1 sun, AM1.5 illumination conditions, with results provided in Table 1, combined with values taken from the literature (for SubPc[11]). OPVs with the structure similar to those used here, utilizing rubrene,[25] tetracene,[26] NPD,[7] and CuPc[22] donors have been reported. The V_{oc}, J_{SC}, FF, and η values presented in Table 1 are consistent with the literature reports (J_S values were not reported). Values of J_{SO} calculated using eq 4 are listed in Table 2. The interface gap, ΔE_{DA}, was calculated using the C_{60} LUMO value (3.5 eV) measured by inverse photoelectron spectroscopy (IPES),[27] and the HOMOs of the donors were obtained both from ultraviolet photoelectron spectroscopy (UPS) and electrochemistry.[28] The calculated V_{oc} values according to eq 5 are also provided in Table 2, along

(25) Taima, T.; Sakai, J.; Yamanari, T.; Saito, K. *Jpn. J. Appl. Phys., Part 2: Lett. Express Lett.* **2006**, *45*, L995–L997.
(26) Chu, C. W.; Shao, Y.; Shrotriya, V.; Yang, Y. *Appl. Phys. Lett.* **2005**, *86*, 243506.
(27) Schwedhelm, R.; Kipp, L.; Dallmeyer, A.; Skibowski, M. *Phys. Rev. B* **1998**, *58*, 13176.
(28) D'Andrade, B. W.; Datta, S.; Forrest, S. R.; Djurovich, P.; Polikarpov, E.; Thompson, M. E. *Org. Electron.* **2005**, *6*, 11–20.
(29) Sato, N.; Seki, K.; Inokuchi, H. *J. Chem. Soc., Faraday Trans. II* **1981**, *77*, 1621–1633.

Table 2. Comparison of Measured and Calculated Performance Parameters[a]

donor	J_{SO}	film	$(nkT)/(q)$ ln $((J_{sc})/(J_{so}))$	$(\Delta E_{DA})/(2q)$	V_{oc} calcd	V_{oc} exptl
SubPc	5.5	Am	−0.02	1.0	0.98	0.97
rubrene	0.43	Am	0.09	0.9	0.99	0.92
NPD	11	Am	−0.10	0.95	0.85	0.85
PtTPBP	12	Am	−0.05	0.7	0.65	0.69
tetracene	150	PC	−0.24	0.80	0.56	0.55
PtOEP	5.1×10^3	PC	−0.40	0.9	0.50	0.52
PdTPBP[b]	9.1	−	−0.082	0.65	0.57	0.61
CuPc	1.5×10^4	PC	−0.41	0.85	0.44	0.48
PtTPNP	62	−	−0.15	0.45	0.30	0.31

[a] J_{SO} are in mA/cm^2, and the remaining data are in V. "Film" refers to the morphology of the donor thin film, as determined by X-ray diffraction, Am = amorphous, PC = polycrystalline.[17,30−36] [b] Illumination intensity = 0.5 suns.

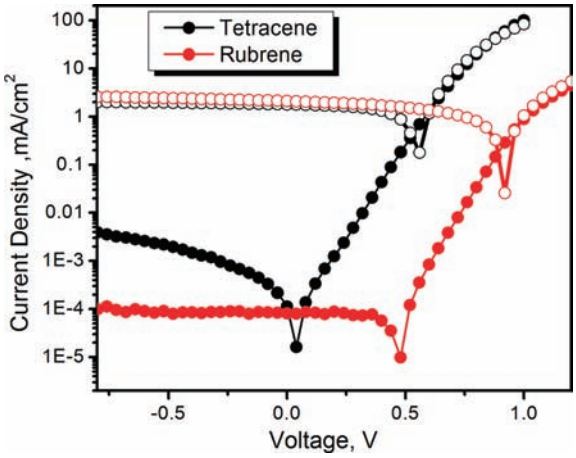

Figure 2. Current density vs voltage characteristics in the dark (closed circles) and illumination under 1 sun, AM1.5 (open circles) conditions for tetracene- and rubrene-based OPVs.

with the measured values for comparison. The calculated V_{oc} closely match those obtained experimentally.

To determine the molecular properties that lead to minimizing J_{SO} for a given ΔE_{DA}, we first consider the donors, tetracene, and rubrene, with results shown in Figure 2 and Table 1. Despite the similarity of the HOMO energies of 5.1 eV for tetracene and 5.3 eV for rubrene,[29] the V_{oc} for the two cells are considerably different at 0.55 and 0.92 V, respectively. The difference in V_{oc} is due to the large difference in the current-dependent terms of eq 5. That is, J_{SO} is 2 orders of magnitude larger for tetracene than for rubrene (see Table 2).

Whereas tetracene is a planar molecule consisting of fused conjugated aromatic rings, the four nearly orthogonal pendant phenyl rings of rubrene prevent close association of the tetracene cores of adjacent rubrene molecules or between the tetracene core and the C_{60} acceptor (see Figure 1), as is evident from comparisons between the solution and thin-film spectra of the two compounds. While rubrene gives similar solution and thin-film spectra, strong intermolecular π interactions in tetracene thin films yield broadened and red-shifted spectrum relative to solution. Weak intermolecular interactions in rubrene decrease both the D/D and particularly D/A interactions relative to tetracene. The weaker D/A interaction in the rubrene-based OPV leads to a correspondingly lower J_{SO}.

The V_{oc} measured for copper phthalocyanine (CuPc)- and platinum tetraphenylbenzoporphyrin (PtTPBP)-containing devices also shows a strong dependence on intermolecular interactions, and thus J_{SO}. The two compounds have comparable π-systems, both with 38 π-electrons. While a larger V_{oc} would be expected for the CuPc-based device due to its higher ΔE_{DA} (ΔE_{DA} = 1.7 eV, vs ΔE_{DA} = 1.4 eV for PtTPBP/C_{60}), the experimental CuPc/C_{60} V_{oc} is actually less than that of PtTPBP by 0.21 V (cf. Table 1). Note that CuPc is a flat molecule with strong intermolecular interactions in the solid state. In contrast, PtTPBP has a highly distorted saddle-shaped conformation with four orthogonal phenyl rings that reduce the availability of the π-system to intermolecular interactions and electronic delocalization.[37] CuPc shows marked broadening of its low-energy absorption in its thin film spectra,[38,39] while the solution and thin film spectra of PtTPBP are the same line width.[30] Added steric bulk, through appended phenyl rings, decreases the degree of intermolecular interaction for PtTPBP relative to CuPc. The high V_{oc} = 0.69 V for the PtTPBP device results from diminished recombination (Figure 3 and Table 2), and hence a lower J_{SO} than for the CuPc device (J_{SO} = 12 and 1.5×10^4 mA/cm^2, respectively).

We have also examined PdTPBP as a donor material. The structure of the Pd analogue is close to that of PtTPBP, where the Pd substitution shifts the HOMO energy slightly, although it does not alter the strengths of the intermolecular interactions. Hence, the Pd and Pt complexes give similar J_{SO} of 9 and 12 mA/cm^2, respectively.

Electronic interactions, or coupling between donor and acceptor molecules, can be modified by varying the strength of the π-conjugation. To explore these effects, we prepared Pt tetraphenyl naphtholporphyrin (PtTPNP, Figure 1), an analogue of PtTPBP whose π-system is extended by benzanulation of four rings onto the benzo moieties of PtTPBP. The lowest energy conformation of the naphthol analog has a saddle shape similar to PtTPBP, resulting from steric repulsions of the meso and pyrolle substituents. The current−voltage characteristics of the

(30) Perez, M. D.; Borek, C.; Djurovich, P. I.; Mayo, E. I.; Lunt, R. R.; Forrest, S. R.; Thompson, M. E. Adv. Mater. 2008.
(31) Gundlach, D. J.; Nichols, J. A.; Zhou, L.; Jackson, T. N. *Appl. Phys. Lett.* **2002**, *80*, 2925–2927.
(32) Mattheus, C. C.; Michaelis, W.; Kelting, C.; Durfee, W. S.; Wöhrle, D.; Schlettwein, D. *Synth. Met.* **2004**, *146*, 335–339.
(33) Mori, T.; Oda, S.; Ooishi, N.; Masumoto, Y. *Jpn. J. Appl. Phys., Part 1: Regul. Pap. Brief Commun. Rev. Pap.* **2007**, *46*, 5954–5959.
(34) Seo, S.; Park, B.-N.; Evans, P. G. *Appl. Phys. Lett.* **2006**, *88*, 232114–3.
(35) Weinberg-Wolf, J. R.; McNeil, L. E.; Liu, S.; Kloc, C. *J. Phys.: Condens. Matter* **2007**, *19*, 276204.
(36) Leznoff, C. C.; Lever, A. B. P. *Phthalocyanines: properties and applications*; VCH: New York, 1989.
(37) Borek, C.; Hanson, K.; Djurovich, P. I.; Thompson, M. E.; Aznavour, K.; Bau, R.; Sun, Y.; Forrest, S. R.; Brooks, J.; Michalski, L.; Brown, J. *Angew. Chem., Int. Ed.* **2007**, *46*, 1109–1112.
(38) Brown, R. J. C.; Kucernak, A. R.; Long, N. J.; Mongay-Batalla, C. *New J. Chem.* **2004**, *28*, 676–680.
(39) Ferreira, J. A.; Barral, R.; Baptista, J. D.; Ferreira, M. I. C. *J. Lumin.* **1991**, *48−49*, 385–390.

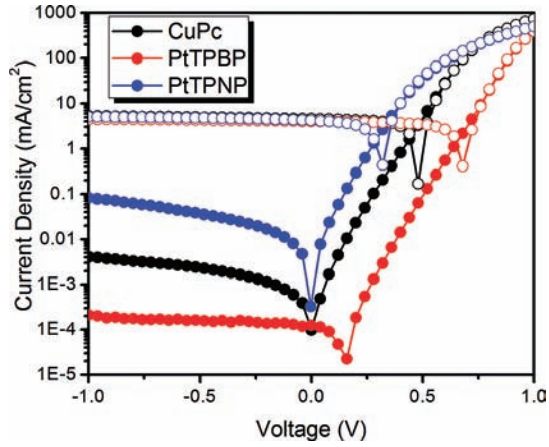

Figure 3. Current density vs voltage characteristics in the dark (closed circles) and illumination under 1 sun, AM1.5 (open circles) conditions for CuPc-, PtTPBP-, and PtTPNP-based OPVs.

PtTPNP donor-containing devices are shown in Figure 3, along with data for PtTPBP- and CuPc-based devices, with their performance provided in Tables 1 and 2. While the PtTPNP- and PtTPBP-based cells have similar photocurrent densities, V_{oc} is reduced to 0.31 V for the PtTPNP device. This low V_{oc} is due to (i) increased π-conjugation of PtTPNP, which reduces the HOMO energy compared to either PtTPBP or CuPc (PtTPNP HOMO energy = 4.4 eV). Hence, the PtTPNP/C_{60} cell has $\Delta E_{DA} = 0.8$ eV, markedly lower than for either PtTPBP or CuPc. (ii) J_{SO} is increased by a factor of 5 for PtTPBP (J_{SO} = 12 mA/cm^2, compared to 62 mA/cm^2 for PtTPNP). The benzannulated rings added to PtTPNP extend beyond the meso-phenyl groups, increasing the $\pi-\pi$ overlap, and thus intermolecular interactions. The resulting increase in J_{SO}, along with its decreased ΔE_{DA}, significantly decrease V_{oc} for this device relative to PtTPBP. While π-expansion leads to an increased J_{SO} relative to PtTPBP, the J_{SO} for PtTPNP is more than 200 times lower than that of CuPc.

To explore planar donors with π-systems of different sizes, Pt octaethylporphyrin (PtOEP) and CuPc were compared (Figure 1).[26] The CuPc π-system is significantly larger than that of PtOEP, which have 38 and 22 π-electrons, respectively. As observed for CuPc, the thin film absorption spectrum of PtOEP shows significant broadening compared to its solution spectrum, which was attributed to aggregate formation.[40] The J_{SO} of CuPc is correspondingly higher than that of PtOEP ($J_{SO} = 1.5 \times 10^4$ and 5.1×10^3 mA/cm^2, respectively), but the difference is not nearly as great as those observed above, consistent with significant steric blocking of the meso phenyls of PtTPBP.

The analysis can be applied to other previously reported donor molecules. For example, *N*,*N*′-bis(naphthalen-1-yl)-*N*,*N*′-bis(phenyl)benzidine (NPD)-based devices (see Figure 1) give V_{oc} = 0.85 V,[7] consistent with $\Delta E_{DA} = 1.9$ eV and reduced recombination losses as reflected by the small J_{SO} =11 mA/cm^2. This value of J_{SO} is similar to that of PtTPBP, indicative of reduced π accessibility and weak interactions with the C_{60} acceptor, due to lose intermolecular packing of the nonplanar NPD molecules. Furthermore, subphthalocyanine (SubPc) exhibits a larger HOMO energy than CuPc, resulting in $\Delta E_{DA} = 1.9$ eV, leading to a high $V_{oc} = 0.97$ V.[11] SubPc has an out-of-plane cone shape whose steric effects reduce intermolecular interactions, and thus recombination at the D/A interface. This gives $J_{SO} = 5.5$ mA/cm^2, which is sufficiently small that it does not significantly influence V_{oc}, as determined from the interface energy gap. SubPc is an example of a donor molecule that comprises features that maximize V_{oc}, a strong absorptivity in the visible, and a high ΔE_{DA} resulting in a low J_{SO}.

The device architecture for the OPVs studied here, i.e., ITO/Donor/C_{60}/BCP/Al, was designed to focus on changes in the donor and at the D/A interface. The acceptor, blocking layer, and cathode materials are kept constant throughout our study. However, as different donors are inserted into the structure, both the D/A and ITO/donor interfaces are affected. While both interfaces could contribute to the observed V_{oc}, the D/A interface dominates in the devices studied here. This was shown by preparing two different devices with a PtTPBP donor, one with the donor in direct contact with ITO and the other with a thin NPD film between ITO and PtTPBP (i.e., ITO/NPD(x Å)/PtTPBP(150 Å)/C_{60}/BCP/Al, $x = 0$, 50). The HOMO level of NPD is 0.5 V below that of PtTPBP. If the ITO/donor interface energetics contributed to the V_{oc} in these devices, a marked shift in the V_{oc} values of the two device is expected. The two devices, with and without the NPD layer, give the same V_{oc} of 0.69 V, supporting our assumption that dark current is limited by recombination at the D/A interface.

X-ray diffraction studies of the donor materials investigated here indicate that both amorphous and polycrystalline thin films are formed, Table 2.[17,30−36] Materials that show evidence of aggregation in thin film absorption spectra, i.e., tetracene, PtOEP, and CuPc, result in polycrystalline thin films. Materials that show little or no evidence of aggregation in their thin film absorption spectra, i.e., SubPc, rubrene, NPD, and PtTPBP, form amorphous thin films. While the strength of intermolecular interactions, via π-system overlap, is only one factor in controlling whether a given material will form an amorphous or polycrystalline film, it is useful to examine the correlation between thin film morphology and J_{SO}. There is a clear distinction in J_{SO} values between the amorphous ($J_{SO} = 1.1 -$ 12 mA/cm^2) and polycrystalline materials ($J_{SO} = 150-1.5 \times 10^4$ mA/cm^2). The $\pi-\pi$ stacking forces that encourage crystal growth likely also leads to strong donor/C_{60} interactions, contributing to the high J_{SO} values observed for the polycrystalline materials.

Conclusions

The correspondence of the calculated values for V_{oc} obtained using eq 5 to experimental values for all D/A materials combinations examined provides evidence for the dependence of the saturation dark current in organic PV cells on the molecular and thin-film structures. Specifically, we show a correspondence between the strength of intermolecular interactions and the saturation current density, reflected in the pre-exponential dark current term, J_{SO}. Weak intermolecular interactions lead to low J_{SO}, and hence correspondingly high open circuit voltages. While not explored in this study, it is reasonable to expect that a similar relationship will be observed for acceptor materials.

It is expected that changes in the OPV architecture will also influence the magnitude of J_{SO}. For example, Li, et al., introduces an electron-blocking layer between the OPV anode contact and donor layer to significantly reduce electron leakage, increasing the V_{oc} by a factor of 2 over analogous devices without the blocking layer.[17] This approach may allow the use of materials with strong intermolecular overlap leading to

(40) Kalinowski, J.; Stampor, W.; Szmytkowski, J.; Cocchi, M.; Virgil, D.; Fattori, V.; Marco, P. D. *J. Chem. Phys.* **2005**, *122*, 154710.

comparatively high J_{SO}, without a marked reduction in open circuit voltage.

To achieve a high open circuit voltage, we find that materials combinations with both a high ΔE_{DA} and low J_{SO} are required. Materials that show weak intermolecular interactions in thin films often result in poor carrier and exciton transport. Since weak intermolecular interactions are also found to result in a low J_{SO}, materials optimized for low dark currents will generally also have short exciton diffusion lengths and poor carrier conductivity, leading to a correspondingly low J_{SC} and FF. These contradictory characteristics would appear to provide a fundamental limit to the ability for a single materials pair to achieve an optimally high V_{oc}, as well as high J_{SC} and FF, needed for high power efficiency. Fortunately, a correlation between low J_{SO} and low J_{SC} and FF is not universaly observed. High power conversion efficiency is possible for OPV materials with sterically inaccessible π-systems or reduced π-extension (low J_{SO}), which have significant overlap between intense absorption bands of the materials and the solar spectrum (high J_{SC}) and good hole conductivity (high FF). Rubrene and PtTPBP donors are examples of such materials, giving relatively high J_{SC} and FF and low J_{SO}. Our work, therefore, can serve as a guide for the molecular design of both D and A materials with improved spectral overlap, while achieving both a low J_{SO} and a high ΔE_{DA}, giving a high V_{oc}.

Experimental Section

The synthesis and characterization of PtTPNP are given in the Supporting Information. PtTPBP and PdTPBP were synthesized according to literature procedures, and purified by vacuum thermal gradient sublimation.[11,30] Copper phthalocyanine (CuPc, 99% pure), PtOEP, tetracene (98%), rubrene (98%), C_{60} (99.5%), and 2,9-dimethyl-4,7-diphenyl-1,10-phenanthroline (bathocuproine, BCP, 96%) were purchased from the Aldrich Chemical Co. and purified by sublimation prior to use. The cathode metal, Al (99.999%), was used as received (from Alrich Chem. Co.).

Photovoltaic cells were grown on solvent-cleaned 150 nm ITO-coated glass substrates with a sheet resistance of 20 ± 5 Ω/sqare, as described elsewhere.[41] The substrates were exposed to UV-ozone for 10 min immediately prior to loading into a high vacuum ($1-3 \times 10^{-6}$ Torr) chamber. Materials were sequentially grown by vacuum thermal evaporation at the following rates: metal-TPBP and PtTPNP (1 Å/s); CuPc, PtOEP, rubrene, NPD, C_{60}, BCP (2 Å/s); and tetracene (15 Å/s). The metal cathodes were evaporated through a shadow mask with 1 mm diameter openings. Current−voltage characteristics of the cells were measured in the dark and under simulated AM1.5G solar illumination using a Keithley 2420 3A Source Meter. Incident power was adjusted using a calibrated Si photodiode to match 1 sun intensity (100 mW/cm^2). Spectral mismatch was calculated to correct the measured efficiencies following standard procedures.[42] Dark current characteristics were fit to eq 2 to obtain J_S, n, and R_s. J_{SO} was calculated using the values for ΔE_{DA} from the literature.

Acknowledgment. This work was supported by Global Photonic Energy Corporation, the Air Force Office of Scientific Research, and the Department of Energy. The authors acknowledge Thin Film Devices, Inc (www.tfdinc.com) for providing ITO.

Supporting Information Available: Details of the PtTPNP synthetic procedure, optical properties (absorption and emission spectra) and electrochemistry of PtTPNP. Spectral response of devices using PtTPNP as donor. This material is available free of charge via the Internet at http://pubs.acs.org.

JA9007722

(41) Burrows, P. E.; Shen, Z.; Bulovic, V.; McCarty, D. M.; Forrest, S. R.; Cronin, J. A.; Thompson, M. E. *J. Appl. Phys.* **1996**, *79*, 7991–8006.
(42) Shrotriya, V.; Li, G.; Yao, Y.; Moriarty, T.; Emery, K.; Yang, Y. *Adv. Funct. Mater.* **2006**, *16*, 2016–2023.